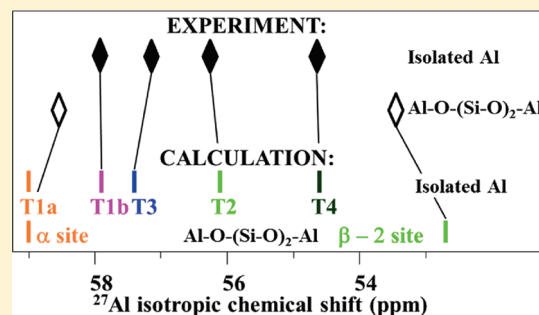


Complex Analysis of the Aluminum Siting in the Framework of Silicon-Rich Zeolites. A Case Study on Ferrierites

Jiri Dedecek, Melissa J. Lucero, Chengbin Li, Fei Gao, Petr Klein, Martina Urbanova, Zdenka Tvaruzkova, Petr Sazama, and Stepan Sklenak*

J. Heyrovský Institute of Physical Chemistry, Academy of Sciences of the Czech Republic, Dolejškova 3, 182 23 Prague, Czech Republic

ABSTRACT: We present a multistep method combining multispectroscopic experiments with DFT calculations to determine the complete Al distribution in silicon-rich zeolites, independent of the presence of Al–O–(Si–O)_n–Al (*n* = 1, 2) sequences in their frameworks. ²⁹Si MAS NMR spectroscopy is employed to confirm the absence of Al–O–Si–O–Al in the framework of silicon-rich zeolites while ²⁷Al 3Q MAS NMR spectroscopy and DFT computations of ²⁷Al isotropic chemical shifts serve to determine the locations of isolated Al atoms. The maximum ion-exchange capacity of zeolites for [Co²⁺(H₂O)₆]²⁺ reveals the presence of close Al atoms (i.e., those Al atoms which are able to balance [Co²⁺(H₂O)₆]²⁺ ions). Then visible spectroscopy of the bare Co(II) ion in the dehydrated zeolite of the samples with close Al is utilized to identify the locations of the corresponding Al–O–(Si–O)₂–Al pairs in a ring. Subsequently, their ²⁷Al isotropic chemical shifts are evaluated at DFT and the complete Al distribution is determined. The complete Al siting in three ferrierite samples with only isolated framework Al atoms and two ferrierites with Al–O–(Si–O)₂–Al sequences was determined. Our results reveal that the Al siting in the former samples varies with the conditions of the zeolite synthesis; Al is present in three or four sites (T1b, T2, T3, and T4) depending on the sample while T1a is never occupied by Al and the concentrations of Al atoms in various T sites are very diverse. For ferrierites with both isolated and close Al atoms, isolated Al atoms occupy the T2, T3, and T4 sites and the close Al atoms are arranged in Al(T1a)–O–(Si–O)₂–Al(T1a) and Al(T2)–O–(Si–O)₂–Al(T2) sequences forming the α and β – 2 cationic sites, respectively. Isolated Al atoms do not occupy the T1b site and close Al atoms do not form Al(T4)–O–(Si–O)₂–Al(T4) sequences of the β – 1 site. The differences between the concentrations of Al in T sites are not as pronounced as those for the ferrierite samples with only isolated framework Al atoms. In addition, our results reveal that the Al siting in ferrierite is not random and depends on the conditions of the zeolite synthesis.



1. INTRODUCTION

Zeolites are crystalline microporous aluminosilicates that are important sorbents and catalysts.^{1–5} Beside the Y and USY zeolites^{6–11} of the faujasite structure, silicon-rich zeolites (Si/Al > 8) such as ZSM-5, the beta zeolite, ferrierite, MCM-22, and mordenite exhibit the highest industrial impact.^{7,11–17} They are regarded to be promising catalysts for synthesis of fine chemicals^{8–10} and in N₂O^{18–25} and NO_x abatement^{26,27} as well as in the processing of biomass.^{28,29} The catalytically active species (protons, metal cations) balance the negative charge of AlO₄[–] tetrahedra. Silicon-rich zeolites exhibit a high number of crystallographically distinguishable framework T sites occupied by Si or Al atoms. This feature, together with a low Al content, leads to a variability of the Al siting (i.e., Al atoms occupy different distinguishable T sites) in the framework.^{30,31} Since countercationic species bind to the AlO₄[–] tetrahedra, the positions of Al in zeolite frameworks control the location of the active sites, which in turn affects the catalytic activity and selectivity. Recently, it has been shown that the Al siting in silicon-rich zeolites is not random and depends on the conditions of the zeolite synthesis.^{30,32} This opens a possibility to tune the Al siting

in the zeolite framework and develop a new generation of highly active and selective catalysts with properties tailored for specific reactions. Determination of the Al siting in the framework is the first and essential step toward synthesis of zeolites with the defined Al distribution. Diffraction techniques cannot distinguish between Al and Si atoms and thus do not allow direct identification of the Al siting in zeolites. However, Olson et al. studied the Cs⁺ siting in extra-framework positions of ZSM-5 by X-ray diffraction and concluded that the three observed Cs⁺ sites indicate a nonrandom Al siting.³³ Similarly, Seff et al. investigated the TI⁺ positions in ZSM-5 and showed that the TI⁺ cations were located in 18 sites with reasonable fractional occupancies, that the Al distribution among the T sites is nonrandom, and that T10 was the most preferred site for Al.³⁴

On the other hand, ²⁷Al solid-state NMR spectroscopy together with DFT calculations gives promising results.^{30,32} However, the presence of Al–O–(Si–O)_n–Al (*n* = 1, 2)

Received: January 11, 2011

Revised: April 22, 2011

Published: May 13, 2011

sequences in the zeolite framework can result in a significant change of ^{27}Al isotropic chemical shift,^{35,36} restricting this approach to matrices containing isolated Al atoms (i.e., zeolite frameworks with the absence of $\text{Al}-\text{O}-(\text{Si}-\text{O})_n-\text{Al}$ ($n = 1, 2$) sequences in a ring). Nevertheless, the presence of $\text{Al}-\text{O}-(\text{Si}-\text{O})_2-\text{Al}$ sequences in the zeolite framework is a standard feature of silicon-rich zeolites even when Si/Al is relatively high (>25).^{37–39}

This paper presents a multispectroscopic approach coupled with DFT calculations that allows for the complex analysis of the Al siting in silicon-rich zeolites independent of the presence of $\text{Al}-\text{O}-(\text{Si}-\text{O})_n-\text{Al}$ ($n = 1, 2$) sequences in the zeolite framework. First, ^{29}Si MAS NMR spectra and the maximum ion-exchange capacity of zeolites for $[\text{Co}^{2+}(\text{H}_2\text{O})_6]^{2+}$ ions of the investigated zeolites are measured. The former serves to confirm the assumed absence of $\text{Al}-\text{O}-\text{Si}-\text{O}-\text{Al}$ sequences in silicon-rich zeolites while the latter reveals the presence of close Al atoms (i.e., those Al atoms which are able to balance $[\text{Co}^{2+}(\text{H}_2\text{O})_6]^{2+}$ ions) in the zeolite frameworks.^{37,40} Then the procedure differs depending on the ion-exchange capacity. Isolated framework Al atoms prevail in the samples having a low ion-exchange capacity and thus a low concentration of close Al atoms. For these samples, determination of the Al siting is based on a comparison of the observed ^{27}Al isotropic chemical shifts obtained by ^{27}Al MQ MAS NMR and those calculated at DFT for isolated framework Al atoms. Samples with a high concentration of close Al atoms also utilize the ^{27}Al MQ MAS NMR procedure, but are further investigated by visible spectroscopy of the bare Co(II) ion in the dehydrated zeolite. This allows identification of rings in the zeolite frameworks with two Al atoms and suggests the siting for the Al atoms in the $\text{Al}-\text{O}-(\text{Si}-\text{O})_2-\text{Al}$ sequences.^{37,40} Their ^{27}Al isotropic chemical shifts are evaluated by DFT. Then the observed ^{27}Al isotropic chemical shifts are compared with those calculated for isolated framework Al atoms as well as Al atoms in the corresponding $\text{Al}-\text{O}-(\text{Si}-\text{O})_2-\text{Al}$ sequences.

This approach is successfully applied to determine the complete Al siting in five ferrierite samples of which two samples contain close Al atoms.

2. EXPERIMENTAL SECTION

2.1. Sample Preparation. We investigated a set of five differently synthesized calcined ferrierite samples (FER/A-FER/E) of various Si/Al ratios. The calcined parent samples, except NH_4 -FER/C, were ion exchanged with 0.5 M NH_4NO_3 twice for 24 h to obtain NH_4 -FER samples which were further equilibrated with 0.5 M NaNO_3 twice for 24 h to get fully ion exchanged Na-FER zeolites. To obtain the concentration of Al pairs and isolated Al atoms in the framework, the five ferrierite samples were equilibrated with $\text{Co}(\text{NO}_3)_2$ solution under the conditions which guaranteed the maximum degree of exchange of the Co(II) cations and the absence of hydrolytic products (0.05 M $\text{Co}(\text{NO}_3)_2$ three times for 24 h). Only Co(II) hexaaqua complexes were exchanged as indicated by UV-vis spectra (not shown in the figures) of Co,Na-FER samples. The Co(II) exchanged samples were thoroughly washed several times with distilled water and dried in open air at room temperature. UV-vis spectra of the dehydrated Co,Na-FER samples indicated that neither bulk Co oxides nor Co oxides well-dispersed in the zeolite framework are present. The introduction of exclusively $[\text{Co}^{2+}(\text{H}_2\text{O})_6]^{2+}$ complexes into zeolites was a necessary condition for obtaining the relevant distribution of framework Al atoms in the samples. Ca,Na-FER zeolites were prepared

Table 1. Chemical Composition of the Ferrierite Samples, the Maximum Ion-Exchange Capacity for $[\text{Co}^{2+}(\text{H}_2\text{O})_6]^{2+}$ Complex ($\text{Co}_{\text{MAX}}/\text{Al}$), and the Relative Concentration of Al Forming $\text{Al}-\text{O}-(\text{Si}-\text{O})_2-\text{Al}$ Sequences

sample	Si/Al	Na/Al ^d	Ca/Al ^b	$\text{Co}_{\text{MAX}}/\text{Al}^c$	Al in $\text{Al}-\text{O}-(\text{Si}-\text{O})_2-\text{Al}^d$ (%)
FER/A ^e	20	1.02	n.d.	<0.03	<5
B ^f	27	0.99	n.d.	<0.02	<5
C ^g	30	1.01	n.d.	<0.02	<5
D ^h	8.6	0.98	0.31	0.33	66
E ⁱ	10.8	0.97	0.11	0.13	26

^a Na-FER samples. ^b Ca,Na-FER samples. ^c Co,Na-FER samples. ^d Values obtained from the analysis of the visible spectra of Co,Na-FER (Al in $\text{Al}-\text{O}-(\text{Si}-\text{O})_2-\text{Al}$ forming the α , β , and γ sites). ^e The Na sample was purchased from Unipetrol, a.s., Czech Republic. ^f The Na-zeolite was synthesized using pure silica (Cab-O-Sil M5), sodium and aluminum sulfate, and NaOH. Pyridine served as the structure directing agent. ^g The NH_4 sample was purchased from Zeolyst International, Inc. ^h The Na,K-sample was purchased from Tosoh Corporation. ⁱ The Na,K-sample was purchased from Unipetrol, a.s., Czech Republic.

employing an ion exchange of the Na-form with 0.5 M $\text{Ca}(\text{NO}_3)_2$ twice for 24 h. The samples were thoroughly washed and then equilibrated on open air at room temperature for several days to guarantee their full hydration for ^{27}Al NMR measurements. The chemical compositions of the ferrierite samples were obtained after their dissolution using atomic absorption spectroscopy (AAS) and X-ray fluorescence spectroscopy (XRF). The chemical composition, the maximum ion-exchange capacity of the ferrierite samples for divalent $[\text{Co}^{2+}(\text{H}_2\text{O})_6]^{2+}$ complexes (see ref 39 for ion-exchange conditions), and their provenance are listed in Table 1. The estimation of the distribution of framework Al atoms by Co^{2+} ions as a probe together with conditions of the ion exchange is described in detail elsewhere.^{37,40} Our XPS measurements reveal only a negligible (<10%) enrichment of the crystal surface (50 Å layer) by Al.

2.2. ^{27}Al and ^{29}Si MAS NMR Spectroscopy. MAS NMR spectra were collected by a Bruker Avance 500 MHz (11.7 T) wide bore spectrometer using 4 mm o.d. ZrO_2 rotors with a rotation speed of 12 kHz for ^{27}Al MAS NMR and 5 kHz for ^{29}Si MAS NMR. ^{27}Al MAS NMR spectra were carried out on fully hydrated Na-FER/A-FER/C. To minimize the effect of a high local concentration of counter cations in the samples with $\text{Al}-\text{O}-(\text{Si}-\text{O})_2-\text{Al}$ sequences, fully hydrated maximum Ca(II) exchanged Ca,Na-FER/D-FER/E were used for ^{27}Al MAS NMR experiments. The ^{27}Al MAS NMR single pulse experiment was performed using high-power decoupling sequence and $\pi/12$ pulse length to enable quantitative analysis of the spectra. Triple quantum (3Q) ^{27}Al MAS NMR experiments were performed using the z -filtered procedure. A $\pi/2$ pulse was used for the excitation and a $\pi/3$ pulse for the conversion. The pulses were individually optimized for each sample. The isotropic chemical shifts were referenced to the aqueous solution of $\text{Al}(\text{NO}_3)_3$. The 2D contour plots presented in Figure 1 are the results of a 2D Fourier transformation followed by a shearing transformation. The isotropic chemical shift was estimated using

$$\delta_{\text{iso}} = (17\delta_{\text{F1}} + 10\delta_{\text{F2}})/27$$

where δ_{F1} is the chemical shift in the isotropic and δ_{F2} is the observed dimension obtained from the spectra simulations. The ^{27}Al 3Q MAS NMR spectroscopy of silicon-rich zeolites is

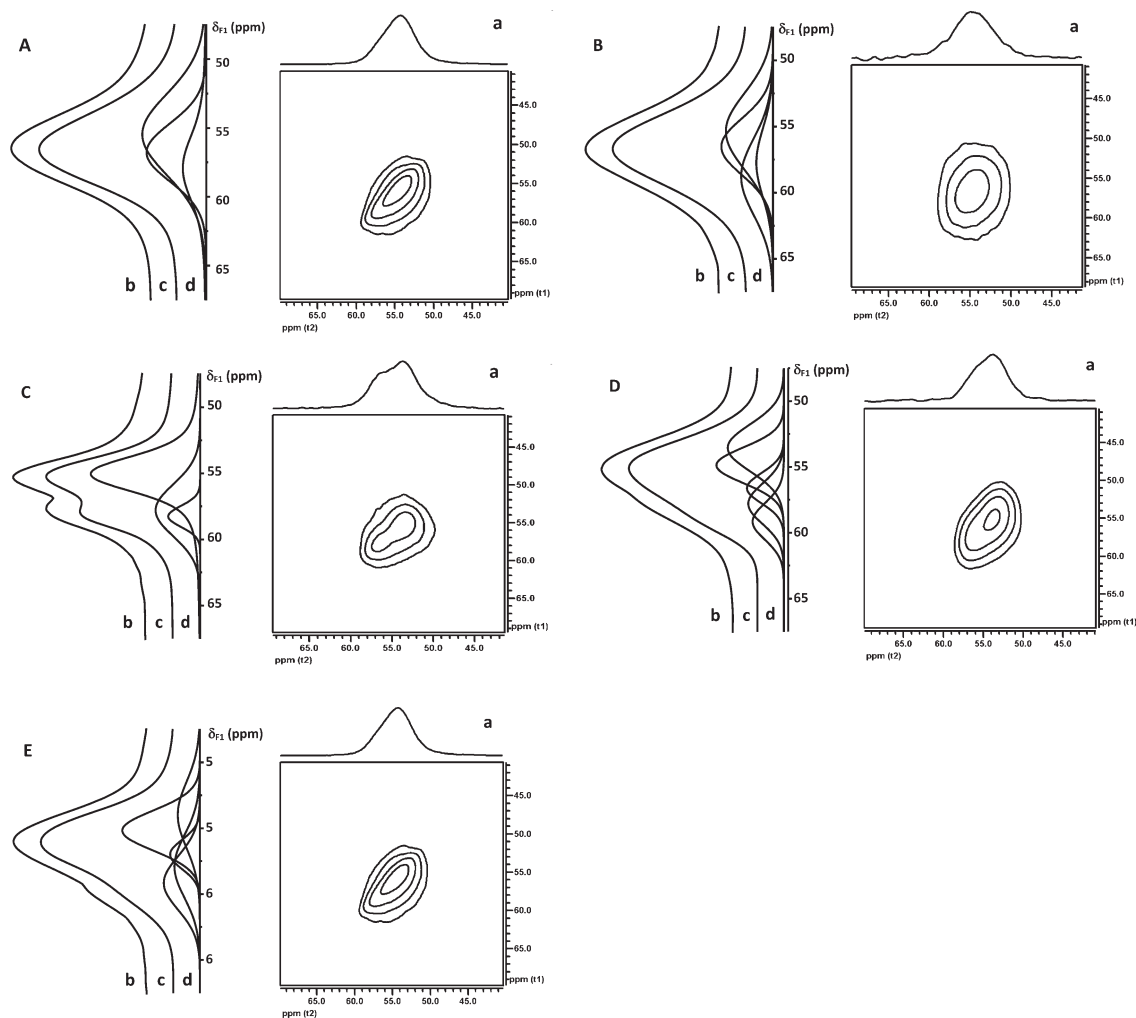


Figure 1. (a) 2D plot of the ^{27}Al 3QMAS NMR spectra of (A) FER/A, (B) FER/B, (C) FER/C, (D) FER/D, and (E) FER/E and F2 projections of the spectra. (b) F1 projections and (c) their simulations using (d) Gaussian profiles.

discussed by van Bokhoven et al.⁴¹ and Sarv et al.,⁴² and the 3Q MAS NMR technique is explained in detail by Alemany.⁴³ F1 and F2 projections, as well as slices of the 2D spectra and single pulse spectra were simulated using dmfit software.⁴⁴

A ^{29}Si MAS NMR high-power decoupling experiment with the $\pi/6$ ($1.7\ \mu\text{s}$) excitation pulse and the relaxation delay of 30 s was applied to collect a single pulse spectrum. The chemical shifts were referenced to Q8M8.

2.3. Visible Spectroscopy of the Co(II) Exchanged Ferrierite Samples. The visible spectra of Co,Na-ferrierites were collected after their dehydration in a vacuum (10^{-3} Pa) at $450\ ^\circ\text{C}$ for 3 h at room temperature using a Perkin-Elmer Lambda 950 UV–vis–NIR spectrometer equipped with a diffuse reflectance attachment with an integrating sphere coated by Spectralon, which also served as a reference. The spectra were processed according to the Schuster–Kubelka–Munk equation. After the baseline correction, the spectra in the region of the d–d transitions were simulated using seven Gaussian bands reflecting the α -, β -, and γ -type Co ions.⁴⁵

3. CATIONIC SITES IN PENTASIL ZEOLITES

Bare divalent metal cations can occupy in pentasil zeolites (e.g., mordenite, ferrierite, ZSM-5, and the beta zeolite) three

types of cationic sites designated as α , β , and γ .^{45–48} The presence of two Al atoms in the site is necessary for stabilization of bare divalent cation.^{37,40,49} These three sites were determined using X-ray diffraction (XRD) for mordenite (sites E, A, and C according to the Mortier notation)^{50,51} and suggested employing UV–vis spectroscopy of bare Co(II) ions as a probe for ZSM-5,⁴⁶ the beta zeolite,⁴⁸ and ferrierite⁴⁵ for which the sites were later confirmed by synchrotron powered XRD.^{52–54} Figure 2 shows the structure of the α and β sites while the γ site is not depicted since the concentration of framework Al atoms forming the γ site in ferrierites is very low⁴⁵ (see section 4.1), and therefore this site is not considered in this study. The α cationic site represents an elongated six-membered ring which is composed of two five-membered rings. This site is easily accessible because it is present on the wall of the main channel in ferrierite. The β cationic site in ferrierite corresponds to a deformed six-membered ring. The β cationic site can be easily reached because it is positioned in an eight-membered ring channel of ferrierite.

4. EXPERIMENTAL RESULTS

4.1. Analysis of the Presence of Al–O–(Si–O)₂–Al Sequences in the Zeolite Framework. The ^{29}Si MAS NMR

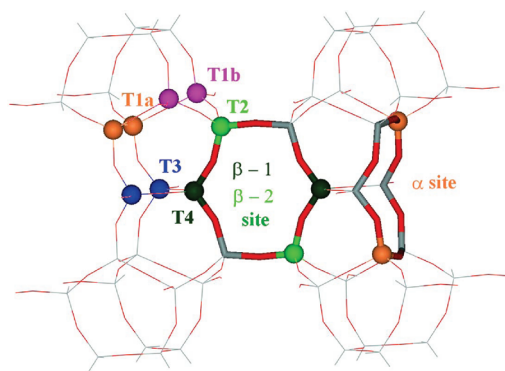


Figure 2. Structure of the α and β sites and the positions of the T1a, T1b, T2, T3, and T4 in the ferrierite framework.

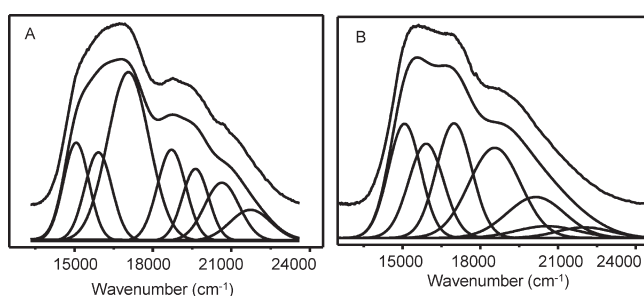


Figure 3. Visible spectra of dehydrated Co,Na-ferrierites and their simulations by Gaussian bands: (A) Co,Na-FER/D; (B) Co,Na-FER/E. The band at 15050 cm^{-1} corresponds to the bare Co(II) ions in the α site, the quartet of bands centered at 15910 , 17020 , 18600 , and 20500 cm^{-1} reflects Co(II) ions in the β site. The doublet of weak bands at 20200 and 21920 cm^{-1} represents a minor fraction of Co(II) ions located in the γ site.

single pulse spectra of the Na-FER samples (not shown in the figures) indicate the absence of Si(2Si,2Al) atoms (i.e., Al–O–Si–O–Al sequences are not present in the framework) for all the samples. This result reveals that only Al–O–(Si–O)₂–Al sequences in a ring and isolated Al atoms exist in the framework of the ferrierite samples used. The ion-exchange capacity of zeolite for [Co²⁺(H₂O)₆]²⁺ complex serves as a measure of close framework Al atoms because isolated Al atoms cannot be balanced by divalent species.^{37,40} Table 1 shows that the FER/A-FER/C samples contain only isolated Al atoms, while close framework Al atoms are present in FER/D-FER/E as both the samples exhibit significant capabilities to accommodate [Co²⁺(H₂O)₆]²⁺ complexes. Our ²⁹Si MAS NMR single pulse experiments revealed that close atoms in the FER/D-FER/E form Al–O–(Si–O)₂–Al sequences (see above). The absence of hydrolytic Co species in the “as prepared” ferrierite samples was confirmed by visible spectroscopy (not shown in the figures).

The ion-exchange capacity of the zeolite for [Co²⁺(H₂O)₆]²⁺ complexes reflects the presence of (1) Al–O–(Si–O)₂–Al sequences located in one ring and (2) two Al atoms which are not present in one ring but they are close enough to accommodate [Co²⁺(H₂O)₆]²⁺ complexes. To distinguish between these two types of close Al atoms, visible spectroscopy of dehydrated maximum [Co²⁺(H₂O)₆]²⁺ exchanged ferrierite samples was applied. Bare Co²⁺ cations are accommodated after

“mild” dehydration (not connected with dehydroxylation or framework perturbations) exclusively in cationic sites containing two framework Al atoms.^{37,40} Thus, the maximum concentration of the bare Co(II) ions (coordinated exclusively to the framework oxygen atoms and charge-balanced by two Al atoms in the samples dehydrated under the conditions described in section 2.3.) in the dehydrated Co,Na-FER zeolites is a measure of the concentration of Al–O–(Si–O)₂–Al sequences in a ring of the zeolite framework.^{37,40} The concentrations of bare Co(II) cations (Table 1) in the ferrierite samples were calculated from the intensities of the d–d transitions (corresponding to a complex band between 12500 and 24000 cm^{-1}) of bare Co(II) ions in the cationic sites. The concentration of Al atoms in Al–O–(Si–O)₂–Al sequences is twice the value of the maximum concentrations of bare exchanged Co(II) ions obtained from the analysis of the d–d transitions in visible spectra.

Analysis of the visible spectra of the maximum Co(II) exchanged FER/D-FER/E samples (Table 1 and Figure 3) shows the presence of bare Co(II) ions in all three cationic sites of ferrierite. The α site is reflected in the band at $15050 \pm 30\text{ cm}^{-1}$; the β site in the bands at 15910 ± 30 , 17020 ± 30 , 18600 ± 40 , and $20500 \pm 80\text{ cm}^{-1}$; and the γ site in the bands at 20200 ± 50 , $21920 \pm 80\text{ cm}^{-1}$. These results fit well with those already reported for Co-ferrierite (15000 ± 100 (α), 16000 ± 100 (β), 17100 ± 100 (β), 18700 ± 200 (β), 20600 ± 300 (β), 20300 ± 100 (γ), and 22000 ± 100 (γ) cm^{-1}).⁴⁵ Using already published concentration coefficients (note that the concentration coefficient of Co(II) in the γ site is four times smaller than those of Co(II) in the α and β sites)⁴⁵ reveal that Al–O–(Si–O)₂–Al sequences are predominantly located in the six-membered rings of the β cationic site ($50 \pm 5\%$ of Al in FER/D and $20 \pm 2\%$ in FER/E) while the rest of them is present in the α site ($10 \pm 2\%$ in FER/D and $7 \pm 2\%$ in FER/E) and their concentration in the γ site is very low ($<5\%$). The total concentration of bare Co²⁺ ions (Co/Al) is estimated to be 0.30 and 0.13 for the Co,Na-FER/D and Co,Na-FER/E samples, respectively. These values are in very good agreement with the results obtained from chemical analysis (Table 1) and thus we conclude that Al–O–(Si–O)₂–Al sequences located in one ring and isolated Al atoms are exclusively present in our samples. Analysis regarding visible spectra of dehydrated Co-zeolites is described in detail elsewhere.^{45–47} The absence of Al–O–Si–O–Al sequences leaves only one possible arrangement of two Al atoms in the α site, while there are two possible locations of two Al atoms forming the $\beta - 1$ and $\beta - 2$ sites (Figure 2).^{55,56}

4.2. ²⁷Al (3Q) MAS NMR Spectra of Zeolites. 2D plots of the ²⁷Al 3Q MAS NMR spectra together with the F1 projections and F1 projection simulations are shown in Figure 1. Three or four distinct ²⁷Al NMR resonances between 54.7 and 58.0 ppm were observed for the samples with only isolated Al atoms (FER/A-FER/C), while five resonances between 53.6 and 58.7 ppm were identified in both the samples with Al–O–(Si–O)₂–Al sequences (FER/D-FER/E). The F1 and F2 values and the isotropic chemical shifts of individual resonances are listed in Table 2. The resonances at 53.6, 54.7, 58.0, and 58.7 ppm exhibit a low dispersion of the isotropic chemical shifts (± 0.1 ppm) for the samples used indicating a high accuracy of the estimation of the isotropic chemical shifts while the NMR parameters of the signals at 56.4 and 57.3 ppm observed for both the samples with as well as without close Al atoms are more scattered, revealing a lower accuracy (± 0.3 ppm) of the estimation of the isotropic chemical shifts. The dispersion of the isotropic chemical shifts

Table 2. NMR Parameters^a of the Individual ²⁷Al Resonances of FER/A-FER/E Determined from 3Q MAS NMR Spectra, Relative Intensity of Individual ²⁷Al Resonances from Single Pulse MAS NMR Spectra, and the T Site Assignment

sample	A	B	C	D	E	average	assignment
Si/Al	20	27	30	8.6	10.8	δ_{iso} (ppm)	
δ_{F1} (ppm)				53.9	54.0		
δ_{F2} (ppm)				52.9	52.8		
δ_{iso} (ppm)				53.5	53.6	53.6 ± 0.1	$\beta - 2$
I_{rel} (%)				36	21		
δ_{F1} (ppm)	55.5	55.4	55.3	55.0	55.2		
δ_{F2} (ppm)	53.8	53.5	53.6	53.9	54.0		
δ_{iso} (ppm)	54.9	54.7	54.7	54.6	54.8	54.7 ± 0.1	T4
I_{rel} (%)	36	45	12	26	40		
δ_{F1} (ppm)	56.8	56.6		56.7	57.0		
δ_{F2} (ppm)	55.0	55.3		56.1	56.1		
δ_{iso} (ppm)	56.1	56.2		56.5	56.7	56.4 ± 0.3	T2
I_{rel} (%)	50	30		10	22		
δ_{F1} (ppm)	57.8	57.8	57.9	57.7	57.9		
δ_{F2} (ppm)	56.3	56.3	56.3	56.8	57.1		
δ_{iso} (ppm)	57.2	57.2	57.3	57.4	57.6	57.3 ± 0.3	T3
I_{rel} (%)	14	19	7	18	6		
δ_{F1} (ppm)		58.7	58.6				
δ_{F2} (ppm)		57.0	57.1				
δ_{iso} (ppm)		58.0	58.0			58.0 ± 0.1	T1b
I_{rel} (%)		6	81				
δ_{F1} (ppm)				59.0	59.1		
δ_{F2} (ppm)				57.9	58.1		
δ_{iso} (ppm)				58.6	58.7	58.7 ± 0.1	T1a, α
I_{rel} (%)				10	11		

^aThe isotropic chemical shifts were referenced to the aqueous solution of $\text{Al}(\text{NO}_3)_3$.

obtained for the five ferrierite samples is slightly worse than that observed for 18 ZSM-5 zeolites ($\leq \pm 0.2$ ppm for most resonances).³² However, it should be noted that close Al atoms were not present in the 18 ZSM-5 samples.³²

4.3. Quantitative Analysis of the Al Siting in Zeolites.

Because the results of multiple-quantum experiments are not quantitative, ²⁷Al single pulse MAS NMR spectra were employed to estimate the Al distribution in the individual T sites. ²⁷Al single pulse MAS NMR spectra of FER/A-FER/E together with the simulation of the spectrum of FER/E with individual components are depicted in Figure 4. The intensities of individual ²⁷Al NMR resonances are listed in Table 2. The spectra simulations reveal three ²⁷Al NMR resonances between 54.7 and 58.0 ppm for the FER/A and FER/C samples, four for FER/B, and five resonances between 53.6 and 58.7 ppm for both the FER/D and FER/E samples with $\text{Al}-\text{O}-(\text{Si}-\text{O})_2-\text{Al}$ sequences.

5. COMPUTATIONAL MODELS AND METHODS

5.1. Computational Model. A bare zeolite framework model, which has been successfully employed in our previous studies,^{30,32,35,36,57} including neither cations nor water molecules is adopted to calculate the local structure around the AlO_4^- tetrahedra and to predict the ²⁷Al NMR shielding. The model features a single Al atom or $\text{Al}-\text{O}-(\text{Si}-\text{O})_2-\text{Al}$ sequence

Table 3. B3LYP GIAO ²⁷Al NMR Shieldings (ppm) and ²⁷Al Isotropic Chemical Shifts (ppm) for (1) Isolated Al Atoms Located in the Distinguishable T Sites of Ferrierite as Well as (2) two Al Atoms Present in $\text{Al}-\text{O}-(\text{Si}-\text{O})_2-\text{Al}$ Sequences Forming the α , $\beta - 1$, and $\beta - 2$ Cationic Sites

T sites	shielding (ppm)	isotropic chemical shift δ_{iso} (ppm)
T1a ^a	512.6	59.0
T1b ^a	513.7	57.9
T3	514.2	57.4
T2	515.5	56.1
T4	517.0	54.6
$\alpha^{b,c}$	512.6	59.0
$\beta - 1^{b,d}$	522.0	49.6
$\beta - 2^{b,e}$	519.0	52.6

^aThe 16-fold T1 site splits into two 8-fold T sites which differ in both the local AlO_4^- geometry—the average $\text{Al}-\text{O}-\text{Si}$ angles are 153.5 and 152.0°—as well as the ²⁷Al isotropic chemical shift. ^bBoth Al atoms have the same shielding/shift. ^cBoth Al atoms are located in T1a. ^dBoth Al atoms are located in T4. ^eBoth Al atoms are located in T2.

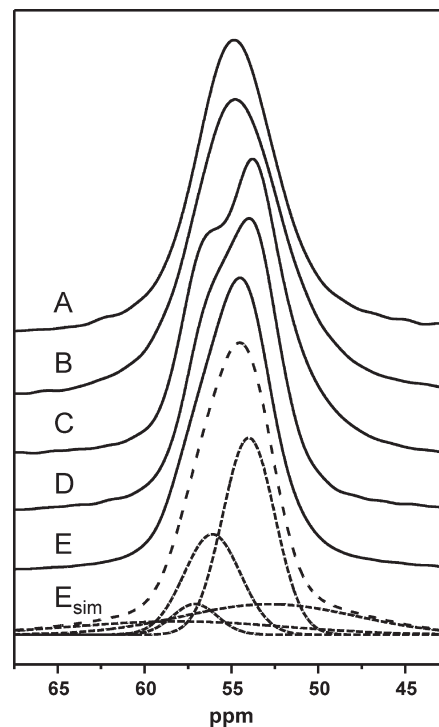


Figure 4. ²⁷Al single pulse MAS NMR spectra of FER/A-FER/E (—) together with the simulation of the spectrum of FER/E E_{sim} (---) with individual components (···).

forming either α or β sites in a unit cell of ferrierite and possesses $P1$ symmetry. Each Al atom bears a formal charge of -1 . The starting structure was downloaded from the zeolite structural database.⁵⁸

5.2. Electronic Structure Calculations and Geometry Optimizations. The CP2K program was employed^{59,60} to fully relax the zeolite unit cells (lattice parameters and geometries) using the BLYP functional,^{61,62} GTH pseudopotentials,^{63,64} and the TZV2P-GTH basis set. Ferrierite structures with (1) a single Al atom ($\text{Si}/\text{Al} = 35$) occupying the crystallographically distinguishable

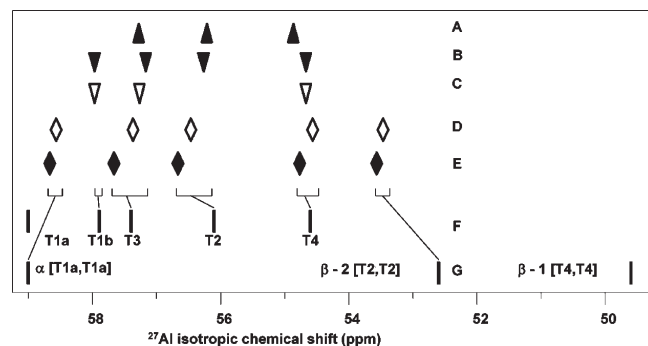


Figure 5. Comparison of the observed (A–E) and calculated (F, G) ^{27}Al isotropic chemical shifts for ferrierites shows the assignment of the ^{27}Al NMR resonances to the T sites. The experimental data for ferrierites (1) with predominantly isolated Al, (A) FER/A, (B) FER/B, (C) FER/C, and (2) with isolated Al as well as $\text{Al–O–(Si–O)}_2\text{–Al}$ sequences, (D) FER/D, (E) FER/E. ^{27}Al isotropic chemical shifts calculated for isolated Al atoms (F), and for $\text{Al–O–(Si–O)}_2\text{–Al}$ sequences in the α and β cationic sites (G).

framework positions (Figure 2) and (2) two Al atoms ($\text{Si/Al} = 17$) forming the α , $\beta - 1$, and $\beta - 2$ cationic sites (Figure 2) were optimized.

5.3. Calculations of ^{27}Al NMR Shielding. Clusters of five coordination shells around the Al atom of interest ($\text{Al–O–Si–O–Si–O–H}_{\text{link}}$) were extracted from the fully relaxed structures to calculate the ^{27}Al NMR shielding by the gauge-independent atomic orbital method (GIAO)⁶⁵ using Gaussian09,⁶⁶ the B3LYP functional,^{62,67} and the pcS basis sets of Jensen⁶⁸—pcS-4 for the Al atom of interest and pcS-1 for all the other atoms. The calculated ^{27}Al shielding values were converted to isotropic shifts (Table 3) using the calculated shielding of $\delta = 571.6$ ppm for $[\text{Al}^{3+}(\text{H}_2\text{O})_6]^{3+}$.⁶⁹

6. COMPUTATIONAL RESULTS

6.1. Ferrierites with only Isolated Al. Our calculations employing one isolated Al atom per unit cell identified five distinguishable structures corresponding to Al substitutions within the four T-sites of the ferrierite framework (Table 3 and Figures 2 and 5). The 16-fold T1 site splits into two 8-fold subsets (T1a and T1b) of the T1 site. T1a and T1b differ in both the local AlO_4^- geometry (the average Al–O–Si angles are 153.5 and 152.0°) as well as the ^{27}Al isotropic chemical shift. The calculated ^{27}Al isotropic chemical shifts reside within the interval from 54.6 (T4) to 59.0 ppm (T1a).

6.2. Ferrierites with Both Isolated Al and $\text{Al–O–(Si–O)}_2\text{–Al}$ Sequences. Our results for the ferrierite structures with two Al atoms in $\text{Al–O–(Si–O)}_2\text{–Al}$ sequences forming the α , $\beta - 1$, and $\beta - 2$ sites are present in Table 3 and Figures 2 and 5. For all three sites, both Al atoms forming $\text{Al–O–(Si–O)}_2\text{–Al}$ have identical NMR shieldings. The presence of an Al atom as a next–next–nearest neighbor does not influence the ^{27}Al isotropic chemical shift of Al forming the α site while it affects Al creating the $\beta - 1$ and $\beta - 2$ sites due to distortions of the local geometry of AlO_4^- tetrahedra. Therefore, ^{27}Al 3Q-MAS NMR spectroscopy enables distinguishing Al of the $\beta - 1$ (the change of the computed ^{27}Al isotropic chemical shift from 54.6 to 49.6 ppm) and $\beta - 2$ sites (from 56.1 to 52.6 ppm) but not Al in the α site.

7. SUGGESTED APPROACH TO IDENTIFY THE AL SITING IN SILICON-RICH ZEOLITES

We propose an approach which combines the previously reported methods for determining the Al siting in silicon-rich zeolites with only isolated framework Al atoms based on the ^{27}Al MAS NMR experiments and DFT calculations of ^{27}Al isotropic chemical shifts^{30,32,57} with (1) ^{29}Si MAS NMR spectroscopy to probe the presence of Al–O–Si–O–Al pairs in the framework and (2) employment of Co(II) ions as probes to examine the presence of $\text{Al–O–(Si–O)}_2\text{–Al}$ sequences and their locations in the zeolite rings.^{37,40} ^{27}Al 3Q-MAS NMR spectroscopy is utilized to distinguish Al atoms with different geometry of AlO_4^- tetrahedra.^{30,32} Al–O–Si–O–Al pairs are usually not present in zeolites with $\text{Si/Al} > 8$;⁷⁰ therefore, ^{29}Si MAS NMR spectroscopy is employed to verify their absence in the investigated samples. The maximum ion-exchange capacity of zeolites for $[\text{Co}^{2+}(\text{H}_2\text{O})_6]^{2+}$ ions can serve as a measure of the concentration of close Al atoms in the framework. The exclusive presence of $[\text{Co}^{2+}(\text{H}_2\text{O})_6]^{2+}$ in the sample is monitored by visible spectroscopy of as-prepared Co-zeolite samples. The $[\text{Co}^{2+}(\text{H}_2\text{O})_6]^{2+}$ species balances two close Al atoms, so the remaining Al atoms correspond to the isolated ones.^{37,40}

7.1. Silicon-Rich Zeolites with Predominant Isolated Framework Al Atoms. When the $[\text{Co}^{2+}(\text{H}_2\text{O})_6]^{2+}$ ion-exchange capacity is low, isolated Al atoms strongly prevail in the zeolite framework. The observed ^{27}Al isotropic chemical shifts can then be compared with those calculated at DFT for computational models of isolated Al atoms occupying all the distinguishable T sites (one Al/Si substitution in the models), providing a means to determine the Al siting within the framework.

7.2. Silicon-Rich Zeolites with Both Isolated Al Atoms and Al Atoms in $\text{Al–O–(Si–O)}_2\text{–Al}$ Sequences. When zeolites exhibit a significant ion-exchange capacity to the divalent complex, visible spectroscopy of the bare Co(II) ion in the dehydrated zeolite is employed to identify rings in the framework with two Al atoms accommodating a bare divalent cation.^{37,40,45} This, in combination with the absence of Al–O–Si–O–Al pairs confirmed by ^{29}Si MAS NMR spectroscopy, suggests the location of the Al atoms in the $\text{Al–O–(Si–O)}_2\text{–Al}$ sequences. The ^{27}Al isotropic chemical shifts are calculated for isolated Al, as well as Al in the proposed $\text{Al–O–(Si–O)}_2\text{–Al}$ pairs for comparison with the experimentally observed shifts measured in this case for the Ca,Na-form to prevent the effect of a high local density of solvated monovalent cations on the local geometry of AlO_4^- in $\text{Al–O–(Si–O)}_2\text{–Al}$. Ca(II) cations compensate for two Al atoms in $\text{Al–O–(Si–O)}_2\text{–Al}$ sequences, while Na^+ cations compensate for isolated Al. Our approach is illustrated in Scheme 1, and its application is demonstrated on the analysis of the Al positions in ferrierites.

8. DISCUSSION

8.1. Determination of the Al Siting in the Ferrierite Samples. Figure 5 compares the calculated and observed ^{27}Al isotropic chemical shifts. Good agreement between the theoretical and experimental shifts allows assignment of the observed resonances to crystallographic sites and supports the applicability of the procedure for locating the positions of Al atoms in silicon-rich zeolites (Scheme 1). The Al siting in FER/A-FER/C varies with the conditions of the zeolite synthesis, and the T1a site is not occupied in FER/A-FER/C. The systematic shift of observed ^{27}Al isotropic chemical shifts of FER/E with respect to those of

Scheme 1. Complex Analysis of the Al Siting in Silicon-Rich Zeolites

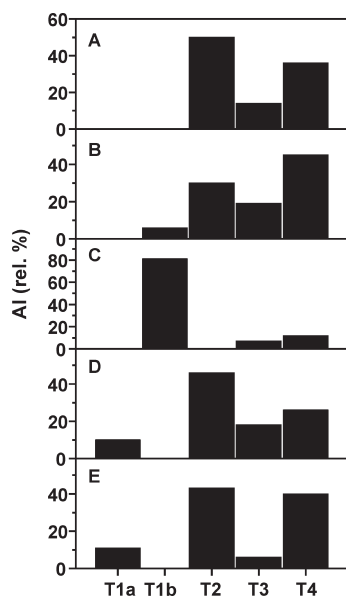
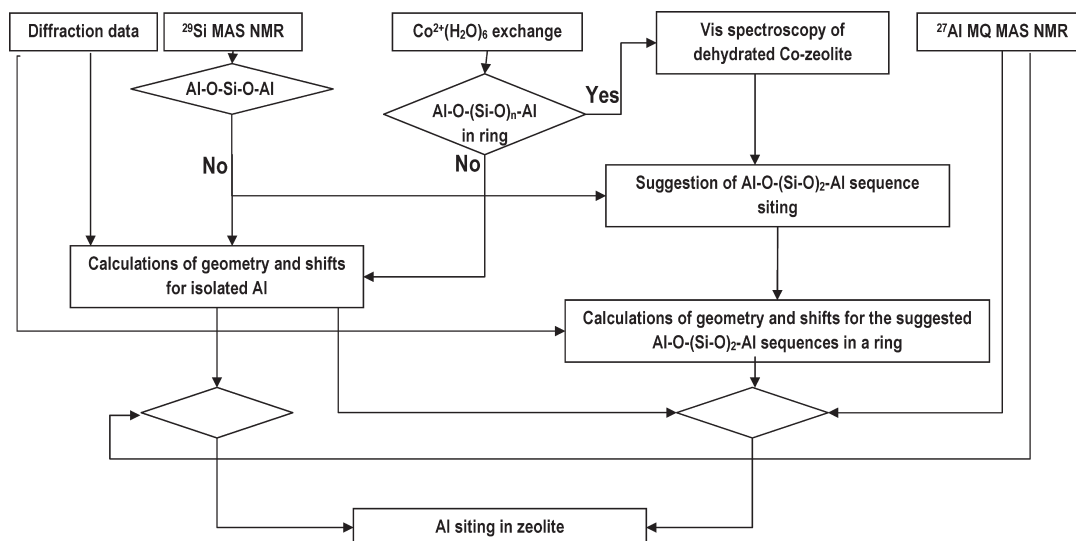


Figure 6. Relative concentration of Al atoms (in %) corresponding to the individual resonances in the FER/A-FER/E samples.

FER/D suggests that the resonance at 57.6 ppm relates to Al in T3. The resonance at 53.6 ppm was observed only in samples with Al–O–(Si–O)₂–Al sequences (FER/D-FER/E) and corresponds to two Al atoms occupying T2 and creating the β – 2 site, while the β – 1 site with two Al atoms in T4 is not formed. The resonance at 58.7 ppm reflects two Al atoms located in T1a, forming the α site. The T1b sites are not occupied by Al in FER/D-FER/E. Figure 5 and Table 2 also reveal that the ²⁷Al isotropic chemical shift corresponding to Al occupying a particular T site depends only weakly on the Si/Al ratio of the sample: all of the ²⁷Al NMR resonances exhibit a low dispersion of the isotropic chemical shifts in the ferrierite samples used.

8.2. Quantitative Analysis of the Al Siting. The concentrations of Al in the T sites obtained from ²⁷Al single pulse experiment are depicted in Figure 6 for the samples used. Note

that the concentration of Al in the T2 site represents the sum of the concentration of Al in the β – 2 site (isotropic shift of 53.6 ppm) and of isolated Al in the T2 site (isotropic shift of 56.4 ppm). Figure 6 clearly shows that the FER/A-FER/C samples differ in the T sites occupied by Al atoms, and moreover, the concentrations of Al atoms in various T sites are very diverse. The concentrations of isolated Al atoms reside within the intervals 6–81%, 6–19%, 30–50%, and 12–45% for the T1b, T3, T2, and T4 sites, respectively. Eighty one percent of Al is located in the T1b site of FER/C and 50% of Al in the T2 site of FER/A revealing that ferrierites with Al siting predominantly in one T site can be synthesized. The differences between the Al occupations are not so pronounced for the FER/D and FER/E samples with Al–O–(Si–O)₂–Al sequences, but the Al distribution significantly varies for the T3 (18 and 6%, respectively) and T4 (26 and 40%, respectively) sites.

It should be noted, that the analysis of the Al distribution in the framework T sites is only semiquantitative due to the strong overlap of the individual resonances and furthermore because of the presence of satellite transitions in the single pulse spectra (the satellite transitions are filtered out in the 3Q experiments). To estimate the accuracy of the concentrations of Al in T sites of the framework of silicon-rich zeolites by ²⁷Al MAS NMR, we compare the concentration of Al obtained from ²⁷Al single pulse MAS NMR spectra for the α site (10 and 11% for FER/D and FER/E, respectively) and the β site (36 and 21% for FER/D and FER/E, respectively) with the corresponding values acquired from the analysis of the visible spectra of Co(II) ions in the α site (10 and 7% for FER/D and FER/E, respectively, see section 4.1) and β site (50 and 20% for FER/D and FER/E, respectively, see section 4.1). Because both the methods provide comparable values, we can estimate that the accuracy of the quantitative analysis of the Al siting by single pulse ²⁷Al MAS NMR is better than ±12%. In addition, since Al atoms in Al–O–(Si–O)₂–Al forming the α site cannot be distinguished from isolated Al atoms in T1a as they have the same isotropic chemical shift of 58.7 ppm (see section 6.2), the concentration of Al related to the resonance at 58.7 ppm corresponds to both isolated Al in T1a and Al in Al–O–(Si–O)₂–Al creating the α site. However, the

concentration of the former Al atoms in FER/D and FER/E is either small or even negligible since the analyses of the visible spectra of Co(II) ions in the α site (giving the concentration of only Al in Al–O–(Si–O)₂–Al) and ²⁷Al single pulse MAS NMR spectra yield very similar results.

8.3. Applicability of the Approach to Identify the Al Siting in Silicon-Rich Zeolites. Our application of the proposed approach on the ferrierite samples results in the determination of the complete Al distribution in silicon-rich zeolites containing also Al–O–(Si–O)₂–Al sequences for the first time to the best of our knowledge. The method is also suitable for any silicon-rich zeolites, regardless of the presence of close Al atoms in their framework. When Al–O–(Si–O)₂–Al sequences are present in the framework of silicon-rich zeolite, then their location is estimated by visible spectroscopy of the bare Co(II) ion in the dehydrated zeolite. Alternatively, IR spectroscopy of skeletal T–O–T vibrations of dehydrated divalent cation (e.g., Mn(II), Mg(II), Ni(II), and Co(II)) exchanged zeolites can be employed to detect the positions of Al–O–(Si–O)₂–Al sequences.^{71,72} The knowledge of the locations of Al–O–(Si–O)₂–Al permits evaluation of the ²⁷Al isotropic chemical shifts using DFT.

Earlier studies^{30,32,35} indicate that for Al–O–(Si–O)₂–Al containing ZSM-5 zeolites additional experimental techniques are necessary to determine the complete Al distribution because the ZSM-5 framework has 24 crystallographically distinguishable T sites and many more possible positions of Al–O–(Si–O)₂–Al. Monitoring the locations of monovalent cations via the vibrational spectra of small adsorbed molecules, with subsequent interpretation through DFT calculations appears to be a reasonable approach.

9. CONCLUSIONS

We present a multistep method allowing determination of the complete Al distribution in silicon-rich zeolites, independent of the presence of Al–O–(Si–O)_n–Al ($n = 1, 2$) sequences in their frameworks. This approach combines multispectroscopic experiments with DFT calculations. ²⁹Si MAS NMR spectroscopy is employed to confirm the absence of Al–O–Si–O–Al in the framework of silicon-rich zeolites while ²⁷Al 3Q-MAS NMR spectroscopy and DFT computations of ²⁷Al isotropic chemical shifts serve to determine the locations of isolated Al atoms. The maximum ion-exchange capacity of zeolites for [Co²⁺(H₂O)₆]²⁺ reveals the presence of close Al atoms. Then vis spectroscopy of the bare Co(II) ion in the dehydrated zeolite of the samples with close Al is utilized to identify the locations of the corresponding Al–O–(Si–O)₂–Al pairs in a ring. Subsequently, their ²⁷Al isotropic chemical shifts are evaluated at DFT and the complete Al distribution is determined.

Comparison of the ²⁷Al isotropic chemical shifts measured for the five ferrierite samples with those calculated at DFT results in assignment of the observed resonances to isolated Al atoms occupying various crystallographically distinguishable T sites and to Al in Al–O–(Si–O)₂–O–Al forming the cationic sites for bare divalent cations. The Al siting in the samples with only isolated Al atoms varies with the conditions of the zeolite synthesis, but T1a site is not occupied. The samples with Al–O–(Si–O)₂–Al sequences located in one ring exhibit both the resonances corresponding to isolated Al atoms occupying T2, T3, and T4 as well as close Al atoms creating the α (pair of Al in T1a) and $\beta - 2$ (pair of Al in T2) sites located in the main and side channels, respectively. Analysis of the ²⁷Al single pulse MAS

NMR spectra of FER/A-FER/E reveals that the concentrations of Al atoms in the distinguishable framework T sites significantly differs. Al atoms of the $\beta - 1$ site (pair of Al in T4) of the side channel are not observed in these samples. Application of our multistep method results in the determination of the complete Al distribution of a silicon-rich zeolite. In addition, our results reveal that the Al siting in ferrierite is not random and depends on the conditions of the zeolite syntheses.

AUTHOR INFORMATION

Corresponding Author

*E-mail: stepan.sklenak@jh-inst.cas.cz.

ACKNOWLEDGMENT

Supported by the Grant Agency of the Academy of Sciences of the Czech Republic (Projects No. IAA400400812, IAA400400908, and IAA400400904), the Grant Agency of the Czech Republic (Project Nos. 203/09/1627 and 203/08/P593), and the Academy of Sciences of the Czech Republic (Project No. KAN100400702).

REFERENCES

- (1) Armor, J. N. *Microporous Mesoporous Mater.* **1998**, *22*, 451.
- (2) Bellussi, G.; Pazzuconi, G.; Perego, C.; Girotti, G.; Terzoni, G. *J. Catal.* **1995**, *157*, 227.
- (3) Chang, C. D. *Catal. Rev. Sci. Eng.* **1983**, *25*, 1.
- (4) Corma, A.; Martinez, A. *Catal. Rev.—Sci. Eng.* **1993**, *35*, 483.
- (5) Csicsery, S. M. *Pure Appl. Chem.* **1986**, *58*, 841.
- (6) Degnan, T. F. *Top. Catal.* **2000**, *13*, 349.
- (7) Marcilly, C. J. *Catal.* **2003**, *216*, 47.
- (8) Clerici, M. G. *Top. Catal.* **2000**, *13*, 373.
- (9) Corma, A.; Garcia, H. *Catal. Today* **1997**, *38*, 257.
- (10) Sheldon, R. A.; Downing, R. S. *Appl. Catal., A* **1999**, *189*, 163.
- (11) Cejka, J.; Perez-Pariente, J.; Roth, W. J. *Zeolites: From Model Materials to Industrial Catalysts*; Transworld Research Network: Kerala, India, 2008.
- (12) Panov, G. I.; Kharitonov, A. S.; Sobolev, V. I. *Appl. Catal., A* **1993**, *98*, 1.
- (13) Shelef, M. *Chem. Rev.* **1995**, *95*, 209.
- (14) Yahiro, H.; Iwamoto, M. *Appl. Catal., A* **2001**, *222*, 163.
- (15) Degnan, T. F. *J. Catal.* **2003**, *216*, 32.
- (16) Schoonover, M. W.; Cohn, M. J. *Top. Catal.* **2000**, *13*, 367.
- (17) Degnan, T. F.; Chitnis, G. K.; Schipper, P. H. *Microporous Mesoporous Mater.* **2000**, *35–6*, 245.
- (18) Jisa, K.; Novakova, J.; Schwarze, M.; Vondrova, A.; Sklenak, S.; Sobalik, Z. *J. Catal.* **2009**, *262*, 27.
- (19) Melian-Cabrera, I.; Mentruit, C.; Pieterse, J. A. Z.; van den Brink, R. W.; Mul, G.; Kapteijn, F.; Moulijn, J. A. *Catal. Commun.* **2005**, *6*, 301.
- (20) Oygarden, A. H.; Perez-Ramirez, J. *Appl. Catal., B* **2006**, *65*, 163.
- (21) Panov, G. I.; Sobolev, V. I.; Kharitonov, A. S. *J. Mol. Catal.* **1990**, *61*, 85.
- (22) Perez-Ramirez, J.; Groen, J. C.; Bruckner, A.; Kumar, M. S.; Bentrup, U.; Debbagh, M. N.; Villaescusa, L. A. *J. Catal.* **2005**, *232*, 318.
- (23) Pieterse, J. A. Z.; Pirngruber, G. D.; van Bokhoven, J. A.; Booneveld, S. *Appl. Catal., B* **2007**, *71*, 16.
- (24) Pirngruber, G. D.; Roy, P. K.; Prins, R. J. *Catal.* **2007**, *246*, 147.
- (25) Roy, P. K.; Prins, R.; Pirngruber, G. D. *Appl. Catal., B* **2008**, *80*, 226.
- (26) Roy, S.; Hegde, M. S.; Madras, G. *Appl. Energy* **2009**, *86*, 2283.
- (27) Forzatti, P.; Nova, I.; Tronconi, E. *Angew. Chem., Int. Ed.* **2009**, *48*, 8366.

- (28) Climent, M. J.; Corma, A.; Iborra, S. *Green Chem.* **2011**, *13*, 520.
- (29) Huber, G. W.; Corma, A. *Angew. Chem., Int. Ed.* **2007**, *46*, 7184.
- (30) Sklenak, S.; Dedecek, J.; Li, C. B.; Wichterlova, B.; Gabova, V.; Sierka, M.; Sauer, J. *Angew. Chem., Int. Ed.* **2007**, *46*, 7286.
- (31) Van Bokhoven, J. A.; Lee, T. L.; Drakopoulos, M.; Lamberti, C.; Thies, S.; Zegenhagen, J. *Nat. Mater.* **2008**, *7*, 551.
- (32) Sklenak, S.; Dedecek, J.; Li, C. B.; Wichterlova, B.; Gabova, V.; Sierka, M.; Sauer, J. *Phys. Chem. Chem. Phys.* **2009**, *11*, 1237.
- (33) Olson, D. H.; Khosrovani, N.; Peters, A. W.; Toby, B. H. *J. Phys. Chem. B* **2000**, *104*, 4844.
- (34) Heo, N. H.; Kim, C. W.; Kwon, H. J.; Kim, G. H.; Kim, S. H.; Hong, S. B.; Seff, K. *J. Phys. Chem. C* **2009**, *113*, 19937.
- (35) Dedecek, J.; Sklenak, S.; Li, C. B.; Wichterlova, B.; Gabova, V.; Brus, J.; Sierka, M.; Sauer, J. *J. Phys. Chem. C* **2009**, *113*, 1447.
- (36) Dedecek, J.; Sklenak, S.; Li, C. B.; Gao, F.; Brus, J.; Zhu, Q. J.; Tatsumi, T. *J. Phys. Chem. C* **2009**, *113*, 14454.
- (37) Dedecek, J.; Kaucky, D.; Wichterlova, B. *Chem. Commun.* **2001**, 970.
- (38) Gabova, V.; Dedecek, J.; Cejka, J. *Chem. Commun.* **2003**, 1196.
- (39) Dedecek, J.; Capek, L.; Sazama, P.; Sobalik, Z.; Wichterlova, B. *Appl. Catal., A* **2011**, *391*, 244.
- (40) Dedecek, J.; Kaucky, D.; Wichterlova, B.; Gonsiorova, O. *Phys. Chem. Chem. Phys.* **2002**, *4*, 5406.
- (41) van Bokhoven, J. A.; Koningsberger, D. C.; Kunkeler, P.; van Bekkum, H.; Kentgens, A. P. M. *J. Am. Chem. Soc.* **2000**, *122*, 12842.
- (42) Sarv, P.; Fernandez, C.; Amoureux, J. P.; Keskinen, K. *J. Phys. Chem.* **1996**, *100*, 19223.
- (43) Alemany, L. B. *Appl. Magn. Reson.* **1993**, *4*, 179.
- (44) Massiot, D.; Fayon, F.; Capron, M.; King, I.; Le Calve, S.; Alonso, B.; Durand, J. O.; Bujoli, B.; Gan, Z. H.; Hoatson, G. *Magn. Reson. Chem.* **2002**, *40*, 70.
- (45) Kaucky, D.; Dedecek, J. I.; Wichterlova, B. *Microporous Mesoporous Mater.* **1999**, *31*, 75.
- (46) Dedecek, J.; Kaucky, D.; Wichterlova, B. *Microporous Mesoporous Mater.* **2000**, *35–6*, 483.
- (47) Dedecek, J.; Wichterlova, B. *J. Phys. Chem. B* **1999**, *103*, 1462.
- (48) Dedecek, J.; Capek, L.; Kaucky, D.; Sobalik, Z.; Wichterlova, B. *J. Catal.* **2002**, *211*, 198.
- (49) Benco, L.; Bucko, T.; Grybos, R.; Hafner, J.; Sobalik, Z.; Dedecek, J.; Hrusak, J. *J. Phys. Chem. C* **2007**, *111*, 586.
- (50) Mortier, W. J. *J. Phys. Chem.* **1977**, *81*, 1334.
- (51) Schlenker, J. L.; Pluth, J. J.; Smith, J. V. *Mater. Res. Bull.* **1978**, *13*, 169.
- (52) Dalconi, M. C.; Alberti, A.; Cruciani, G. *J. Phys. Chem. B* **2003**, *107*, 12973.
- (53) Dalconi, M. C.; Alberti, A.; Cruciani, G.; Ciambelli, P.; Fonda, E. *Microporous Mesoporous Mater.* **2003**, *62*, 191.
- (54) Dalconi, M. C.; Cruciani, G.; Alberti, A.; Ciambelli, P.; Rapacciuolo, M. T. *Microporous Mesoporous Mater.* **2000**, *39*, 423.
- (55) Benco, L.; Bucko, T.; Grybos, R.; Hafner, J.; Sobalik, Z.; Dedecek, J.; Sklenak, S.; Hrusak, J. *J. Phys. Chem. C* **2007**, *111*, 9393.
- (56) Sklenak, S.; Andrikopoulos, P. C.; Boekfa, B.; Jansang, B.; Novakova, J.; Benco, L.; Bucko, T.; Hafner, J.; Dedecek, J.; Sobalik, Z. *J. Catal.* **2010**, *272*, 262.
- (57) Sklenak, S.; Dedecek, J.; Li, C. B.; Gao, F.; Jansang, B.; Boekfa, B.; Wichterlova, B.; Sauer, J. *Collect. Czech. Chem. Commun.* **2008**, *73*, 909.
- (58) <http://www.iza-structure.org/databases/> space group, *Immm*; cell parameters, $a = 19.018$, $b = 14.303$, $c = 7.541$ Å.
- (59) VandeVondele, J.; Krack, M.; Mohamed, F.; Parrinello, M.; Chassaing, T.; Hutter, J. *Comput. Phys. Commun.* **2005**, *167*, 103.
- (60) The CP2K developers group, <http://cp2k.berlios.de>, 2010.
- (61) Becke, A. D. *Phys. Rev. A* **1988**, *38*, 3098.
- (62) Lee, C. T.; Yang, W. T.; Parr, R. G. *Phys. Rev. B* **1988**, *37*, 785.
- (63) Hartwigsen, C.; Goedecker, S.; Hutter, J. *Phys. Rev. B* **1998**, *58*, 3641.
- (64) Krack, M. *Theor. Chem. Acc.* **2005**, *114*, 145.
- (65) Wolinski, K.; Hinton, J. F.; Pulay, P. *J. Am. Chem. Soc.* **1990**, *112*, 8251.
- (66) Frisch, M. J.; et al. *Gaussian 09, Revision A.02*; Gaussian, Inc.: Wallingford, CT, 2009.
- (67) Becke, A. D. *J. Chem. Phys.* **1993**, *98*, 5648.
- (68) Jensen, F. *J. Chem. Theory Comput.* **2008**, *4*, 719.
- (69) The geometry of $[\text{Al}^{3+}(\text{H}_2\text{O})_6]^{3+}$ was optimized at B3LYP/cc-pVQZ. The Al NMR shielding of 571.6 ppm was obtained at B3LYP employing the pcS4 basis set for Al and pcS1 for the other atoms.
- (70) Takaishi, T.; Kato, M.; Itabashi, K. *Zeolites* **1995**, *15*, 21.
- (71) Sobalik, Z.; Tvaruzkova, Z.; Wichterlova, B. *J. Phys. Chem. B* **1998**, *102*, 1077.
- (72) Drozdova, L.; Prins, R.; Dedecek, J.; Sobalik, Z.; Wichterlova, B. *J. Phys. Chem. B* **2002**, *106*, 2240.